1. Publication Nº INPE-3723-RPE/497
2. Version
3. Date November 1985
5. Distribution ☐ Internal ☒ External ☐ Restricted
4. Origin DME
Program TECLIM
6. Key words - selected by the author(s)
TROPICAL HEAT SOURCE
DROUGHT IN NORTHEAST BRAZIL
CLIMATE MODELING
7. U.D.C.: 551.577.38(8)

8. Title INPE-3723-RPE/497

TRANSIENT CONVECTION OVER THE AMAZON/BOLIVIA REGION AND THE DYNAMICS OF DROUGHT OVER NORTHEAST BRAZIL

10. Nº of pages: 31
11. Last page: 29
12. Revised by
Carlos A. Nobre
13. Authorized by
Marco Antonio Raupp
Director General

9. Authorship
Julio Buchmann (*)
Pedro Leite da Silva Dias (**)
Antonio Divino Moura
Responsible author

14. Abstract/Notes

A two-layer, nonlinear, equatorial β-plane model, in p-coordinates is used to study the atmospheric response to a large scale prescribed heat source varying in time. The heat source is meant to represent a convective burst with total duration of approximately 48 hours over the Amazon/Bolivia region. The boundary conditions used are meridional velocity zero at 60°S, $\omega = 0$ at the top and zero geometric velocity at the lower boundary. Sensitivity study was done which includes initial state at rest, compared with realistic initial flow. The scale of the heat source is 1500km in latitude and longitude and it is centered at 10°S. Special attention is paid to the distribution and intensity of the induced vertical motion. The model is integrated for two days and the preliminary results show agreement with the observed 200mb flow. Of interest is the establishment of a trough and descending motion to the northeast of the heat source. A conjucture is thus made that the Amazon heat source and its fluctuations bear some relationship with the drought problem over Northeast Brazil.

15. Remarks Archives for Meteorology, Geophysics, and Bioclimatology - Springer-Verlag, Wien I, Mölker Bastei 5, A-1011 Wien/Postfach 367.
(*) UFRJ - Universidade Federal do Rio de Janeiro
(**) IAG - Instituto Astronômico e Geofísico da USP

TRANSIENT CONVECTION OVER THE AMAZON/BOLIVIA REGION AND THE DYNAMICS OF DROUGHTS OVER NORTHEAST BRAZIL

J. Buchmann[1], P.L. da Silva Dias[2], and A.D. Moura[3]

With 12 figures

1. Departamento de Meteorologia - UFRJ, 22910, Rio de Janeiro, Brazil.
2. Instituto Astronomico e Geofisico - USP, 01051, Sao Paulo, Brazil.
3. Instituto de Pesquisas Espaciais/CNPq, 12200, Sao Jose dos Campos, Brazil.

ABSTRACT

A two-layer, nonlinear, equatorial β-plane model, in p-coordinates is used to study the atmospheric response to a large scale prescribed heat source varying in time. The heat source is meant to represent a convective burst with total duration of approximately 48 hours over the Amazon/Bolívia region. The boundary conditions used are meridional velocity zero at 60^{o}N and 60^{o}S, $\omega = 0$ at the top and zero geometric velocity at the lower boundary. Sensitivity study was done which includes initial state at rest, compared with realistic initial flow. The scale of the heat source is 1500km in latitude and longitude and it is centered at 10^{o}S. Special attention is paid to the distribution and intensity of the induced vertical motion.

The model is integrated for two days and the preliminary results show agreement with the observed 200mb flow. Of interest is the establishment of a trough and descending motion to the northeast of the heat source. A conjecture is thus made that the Amazon heat source and its fluctuations bear some relationship with the drought problem over Northeast Brazil.

1. Introduction

The Northeast Brazil climate has been the subject of study by scientists, who have been trying to explain the observed climatic anomalies due to the disruption of the lives of over 30,000,000 people. Two main lines of research have been followed. The first one considers possible local effects as the main cause of the anomaly. Along this line, Gomes Filho [4] studied two mechanisms of formation and maintenance of the semiarid region: albedo gradients and orographic effects. However this conclusion is not well established yet. Along the second line of research, the main cause is due to external mechanisms such as those invoked by Namias [16], Hastenrath and Heller [8], Kousky [11], Moura and Shukla [15] and Buchmann [2]. Namias [16] demonstrated a connection between the 700mb circulation pattern over the North Atlantic and the rainfall at Quixeramobim (state of Ceará). Hastenrath and Heller [8] used a large number of observations to show that rainfall in the region of Ceará is closely linked to the meridional displacement of the equatorial trough zone. Kousky [11] showed that: a) frontal systems penetrate the southern part of Northeast Brazil throughout the year; b) frontal incursion plays an important role in the December-January maximum in the month precipitation in the southern part Northeast Brazil; c) in certain periods, the frontal incursions affect rainfall as far north as Ceará. Moura and Shukla [15] proposed that a possible mechanism for the occurrence of severe droughts over Northeast Brazil is the establishment of a thermally direct local circulation which has the ascending branch at about 10^{o}N and the descending one over Northeast Brazil and the adjoining oceanic region. Buchmann [2] studied the occurrence of drought and rain anomalies in the Northeast Brazil, in relation to variations in the synoptic pressure systems located in middle latitudes of the Northern Hemisphere, through the mechanism of lateral forcing.

However, there are other mechanisms not yet fully explored. Because the amount of latent heat released during the rainy season of the Amazon region is so large (Kasahara and Mizzi, [9]), one can expect a significant effect of the local forced circulation on the neighboring regions, and assume a direct thermal circulation established over the tropical sector of South America, with maximum upward movement over the Amazon region and the downward branch of the resulting Walker circulation affecting Northeast Brazil and the adjacent Atlantic Ocean (Gill, [3]). This hypothesis agrees with Bjerknes [1] and Kidson [10] ideas concerning the relationship between the upper tropospheric high (also known as Bolivian High after Gutmann and Scwerdtfeger, [5]), and the variability of precipitation over Northeast Brazil. Specifically, the circulation pattern over South America shows large variations in different time scales: (i) from the Southern Hemisphere summer to winter, the 200mb circulation changes from a well-defined upper tropospheric anticyclone to near equatorial westerlies (Kruels et al., [13]); (ii) convective bursts during summer make a substantial rearrangement of the upper trospospheric anticyclone and the accompanying through over Northeast Brazil (Silva Dias et al., [19] ; Virgi, [21]), and (iii) the large diurnal variation of convection seems to have a strong signal in the divergent component of the upper tropospheric circulation (Silva Dias et al., [20]). Latent heat release is a plausible controlling mechanism on the three time scales of the tropical tropospheric circulation over South America. Due to the confinement of the precipitation pattern in the central and western part of Brazil during the summer months, it is reasonable to investigate the effect of latent heat-induced circulations on Northeast Brazil.

Fig. 1a shows a typical infrared satellite image with the well-developed convection over the Amazon region. Fig. 1b shows the associated 200mb streamlines and the vertical pressure velocity field (ω) at 500mb (thin solid and dashed lines for upward and downward motion, respectively), as obtained from the National Meteorological Center (NMC) analysis for January 5, 1981. Similar upper tropospheric situations as well as the transient behavior are shown in Fig. 6 of Silva Dias et al. [19] . Upward vertical motion is observed in association with the upper tropospheric circulation and sinking motion occurs over Northeast Brazil when the upper circulation is cyclonic. The satellite imagery qualitatively agrees fairly well with the NMC vertical motion. In particular, recent model studies by Silva Dias et al. [19] indicated that transient convection on the typical time and spatial scales over the Amazon region tend to generate a Walker-type circulation associated with Kelvin waves to the east of the heat source, an upper tropospheric anticyclone centered to the southwest of the source and an upper trough over Northeastern Brazil in agreement with the observed pattern shown in Fig. 1. However, the model results were based on the linearized shallow water equations about a basic state at rest. The objective of this paper is to further explore the response of the atmosphere to transient forcing, in terms of the associated vertical motion and possible nonlinear effects with a two-level primitive equation model. The time and horizontal scales of convective bursts, centered at about 10°S, are assumed to be of approximately 48 hours and of the order of 1500 km, respectively.

2. Observational Evidence

The summer upper level circulation over tropical South America is characterized by the anticyclonic flow with large transient variations (Virji, [21]). In order to analyse the transient behaviour of the upper circulation and its association with cloudiness, we obtained the vertical motion at 500mb at 00:00 GMT and 12:00 GMT for January, 1981, based on the NMC analyses. This choice was based on the particularly intense convective activity observed in the period (Silva Dias et al., [20]). A mass balanced kinematic method between 1000mb and 200mb is applied to the gridded data (horizontal resolution of approximately $5^{o} \times 5^{o}$). Infrared geostationary images processed by the Instituto de Pesquisas Espaciais - INPE (Institute for Space Research) were collected for January, 1981 at times as close as possible to 00:00 GMT and 12:00 GMT.

The diurnal signal in the vertical motion is clearly evident during the period with maximum upward motion at 00:00 GMT over the Amazon region and Central Brazil (approximately 20:00 LT). The diurnal variation in the vertical motion field (ω in pressure vertical coordinate) over tropical South America has been studied by Silva Dias et al. [20], who showed that the signal is significant from a statistical point of view. However, as noticed by Virji [21], convective bursts often occur over tropical South America, frequently in response to penetrating mid latitude systems (Kousky and Virji,[22]). One such sequence of satellite images (Fig. 2) was observed from the 22nd to the 25th of January, 1981 with enhanced convective activity on the 23rd, as shown in the infrared satellite image at 21:16 GMT

(Fig. 2.b). Fig. 3 shows the accompanying upper level wind vectors (200mb) and the 500mb vertical motion (solid lines for $\omega \geq 0$ and dashed lines for $\omega < 0$). A comparison between the computed vertical motion and convective activity (Fig.3 and 2,respectively) shows a reasonable agreement, with maximum upward vertical motion at 00 GMT on the 24th (Fig. 3c for the ω-field and Fig. 2b for the satellite image).

Several interesting points deserve attention in Fig. 3: (i) before the convective burst,the anticyclonic circulation is zonally elongated towards the west with center at approximately 18^oS and 75^oW (Fig. 3a); (ii) as the convective activity enhances, a strong cross equatorial flow over the northern Amazon region is observed (Fig. 3c), accompanied by enhanced upward vertical motion over Central Brazil (10^oS, 55^oW); (iii) as the convective activity decreases, the easterly component is established just off the equator (Fig. 3f); (iv) the center of the anticyclonic circulation is displaced eastward as the convective activity enhances (Fig. 3a to 3c), presenting a westward elongation after the maximum activity (Fig. 3e and 3f); (v) ridging is observed (25^oS, 55^oW) during the final period (Fig. 3e and 3f) just south of the most active region. These general observations were also detected in other periods of January 1981 and during a particular period of February 1979 (8th to 12th) as discussed by Silva Dias et al. [19] .

3. Governing Equations

The fully nonlinear primitive equations above an equatorial β-plane are discretized in the vertical assuming a two-level model, with the zonal and meridional wind components and potential temperature defined at 750mb and 250mb. The geopotential and vertical pressure velocity are defined at the bottom pressure level (1000mb), 500mb and top (0mb). The vertical boundary conditions are $\omega = 0$ at the top and zero geometrical velocity at the lower boundary ($W = 0$). No topographic effects are included. Thus, there are two vertical modes in the linearized version of this model (about a basic state at rest): the external (barotropic) and the internal mode with reversing sign in the vertical (baroclinic). Schuman's horizontal discretization scheme is applied to the governing equations (Haltiner, [7]) and the time differencing scheme is centered in time. The horizontal boundary conditions are constant in time with $v = 0$ at 60^oN and 60^oS. Zonal periodicity at the equatorial circumference of the earth is also assumed. The horizontal boundary conditions are not expected to influence the model results because the time scale of the integration is sufficiently short to avoid boundary contamination.

The model circulation is forced by a known heat source which is Gaussian-shaped in the horizontal direction and with time dependence as shown in Fig. 4, with maximum heating at 24 hours. In the particular case of the two level model, the heat source is assumed to have the same intensity at 750mb and 250mb, corresponding to 6^oC/day. The choice of the spatial and temporal scales are based on the satellite imagery. The heat source intensity is, however, an estimate based on observations in other tropical regions (Riehl, [17]) because there are no aerological estimates of the transient characteristics of the Amazon heat source, to the authors' knowledge.

The results shown in this paper are confined to the model outputs at 24 and 48 hours. No initial instabilities were observed in the model integration because the transient forcing is slowly increasing in time rather than a switch-on forcing. A carefull observation of the vertical motion field at frequent intervals (4 hours) shows a very stable and continuous evolution of the numerical solution.

Numerical solutions including Rayleigh damping and Newtonian cooling were obtained using a characteristic time scale of 10 days. Although the flow intensity was somewhat reduced compared to the frictionless version, no major discrepancies were observed up to 2 days of integration time. Constant radiative cooling of 1.5^{o}C/day was also tested in the model. Since no available potential energy is generated in this case and the model contains no moisture physics or radiation interaction, no horizontal motion is generated by such forcing. In fact, the prescribed heat source can be interpreted as the combination of both latent heat release and radiative vertical flux divergence is certainly an important process (Gray and Jacobson, [6]) due to the typical difference between the vertical profiles of clear air/cloudy stay radiative cooling rates. In order to keep the thermal balance, clear regions are associated with sinking motion which approximately balances the radiative cooling. Horizontal motion is also generated by the difference between the radiative cooling rates in cloudy and clear regions, but this effect is included in the prescribed heat source. Thus, the results shown below correspond to the frictionless adiabatic version.

4. Model Results

Silva Dias et al. [19] computed how the forced energy is partitioned between Kelvin, mixed Rossby-gravity, Rossby and gravity modes for the linearized primitive equations about a basic state at rest assuming different temporal and spatial scales for the heat source. The characteristics of the response are quite different from the stationary forcing (Gill, [3] ; Moura and Shukla, [15]). The main findings are: (i) Rossby wave energy increases as the spatial scale and the latitude of the forcing increases; (ii) as the forcing time scale decreases, less energy is excited in the high frequency modes; (iii) as the forcing spatial scale increases, the energy in gravity modes decreases sharply ; (iv) for fixed time scale of the forcing, the energy in high frequency modes initially increases with the horizontal scale of the forcing and then decreases.

The results obtained with the two-level nonlinear primitive equation model are essentially similar to the linear situation shown in Silva Dias et al. [19] , primarily concerning the rotational contribution and the Kelvin component to the east of the source. Figs. 5 and 6 show the 250mb wind field at 24 and 48 hours, respectively, for a heat source centered at 10^{o}S, with symmetrical e-folding width of the order of 1500km. The corresponding vertical motion field at 500mb is shown in Figs 7 and 8. The development of the upper tropospheric anticyclone and the trough over Northeast Brazil is well depicted by the model (compare with Fig. 4 of Silva Dias et al.[19]). The heating over the Amazon region initially induces subsidence over Northeast Brazil, although the forcing function is quite wide. It is interesting to note the preferred location of the downward motion. As time increases, a slight ascending motion can be detected over Northeast Brazil. However, with smaller scale forcing, the subsidence over this region is emphasized as shown in the vertical motion field at 24 hours for a heat source located at $15^{o}S$ and with a meridionally elongated source (zonal and meridional e-folding width of 700 km and 1500 km, respectively), as shown in Fig. 9.

Possible nonlinear effects were also studied by prescribing an initial condition with a more realistic zonal flow with subtropical jets located at about 35^{o} to the north and south of the equator, attaining 35 ms^{-1}. In this case the wind field at 48 hours at 250mb is shown in Fig. 10 and the deviation from the initial flow is shown in Fig. 11. The basic characteristics of the forcing are the same of Figure 6. The main difference from the no initial flow case is due to the stronger meridional component to the south of the upper anticyclone. This effect implies a larger distortion of the zonal flow (ridging) and therefore we might expect important downstream amplification of the wave train if longer time scale forcing is applied or if a succession of convective bursts occurs (Lau and Lim, [14]). The upper westerlies to the east of the heat source are also evident in Figs. 5, 6, 9 and 10. This upper level configuration seems to be related to free Kelvin modes according to Silva Dias et al., [19] and recently found in satellite data by Salby et al [18] .

The model results seem to corroborate observed characteristics of the tropospheric circulation over tropical South America during actively convective episodes, as presented in Section 4. In particular, there is correspondence with the intense cross equatorial flow at the initial stages of the forcing (Fig. 5), the slow turning of the wind to easterlies south of the equator (Fig. 6) and the westward displacement of the upper anticyclone center at the latter stages (Fig. 6). The case with initial zonal flow indicates that nonlinear interactions might be relevant in emphasizing the observed ridging at the final stages of the convective burst,as observed in Figs. 3e e 3f.

5. Conclusion

The nonlinear primitive equation model simulation of the transient heat source reproduced most of the results obtained with the linear shallow water equations of Silva Dias et al. [19] . However, the results also indicate that the induced subsidence occurs preferentially over Northeast Brazil primarily for meridionally elongated heat sources. These results indicate that a regional Walker type circulation with ascending motion over Northeast Brazil may take place. Thus, excessive convection over central and western South America may induce an unfavourable dynamical situation for convection over the Northeast region. The model is able to simulate the basic features of the observed characteristics of the transient convection episodes (Section 2). The nonlinear effects up to 2 days seem to be confined to higher latitudes where the upper anticyclonic circulation interacts with the upper westerlies, intensifying the ridging mechanism. The intensification of the equatorial westerlies to the east of the forcing (Fig. 6)doesnot seem to be evident in the observations (Fig. 3) although westerlies are observed. This can be due to the rotational constraints imposed on the analyses and assimilation scheme used by NMC. It is interesting to note that transient forcing is more realistic than stationary forcing over tropical South America. According to the linear model partition of energy, discussed in the previous section, more energy in fast modes is expected for highly transient forcing and therefore more intense vertical motion teleconnections are expected through gravity wave activity.

Similar model simulations have also been performed with zonally elongated heat sources located over the eastern equatorial Pacific Ocean. These model results are expected to represent the El Niño type of anomaly. The model results also seem to indicate a preferred subsidence region over most of equatorial South America on the time scale of two days (Fig. 12). These results are in agreement with the observed negative correlation between precipitation over the eastern Pacific Ocean and over tropical South America (Kousky et al., [12]).

ACKNOWEDGEMENTS

The authors are grateful to Dr. Vernon E. Kousky, Mr. J.P. Bonatti, Mr. Manoel A. Gan and Mrs. Iracema F. Cavalcanti. Research support was available through FINEP grants to INPE and IAG-USP. Partial support for this work was provided by NASA grant NAG 5-127. The first author also benifitted from a post-doctoral fellowship provided by CNPq. We are also grateful to Dr. C. Nobre for editorial comments and suggestions.

References

[1] Bjerkness, J. : Atmospheric teleconnections form the equatorial Pacific. Mon. Wea. Rev., 97, 163-172, 1969.

[2] Buchmann, J.: A study of the influence of extratropical meteorological phenomena on climatic variability in northeast Brazil. Doctoral dissertation presented at COPPE/UFRJ, 123 pp [available from COPPE/UFRJ - C.P. 1191, 20000 - RJ, Brazil] (in Portuguese), 1981.

[3] Gill, A.E.: Some simple solutions for heat induced tropical circulation. Quart. J. Roy. Meteor. Soc., 106, 447-462, 1980.

[4] Gomes Filho, M.F.: A study of differential albedo and orographical influence on the atmospheric circulation: Application to Northeast Brazil. Master thesis presented at the Institute for Space Research, INPE. INPE-1640-TDL/015, 86 pp [Available from INPE - C.P. 515, 12200 São José dos Campos, SP, Brazil] (in Portuguese), 1979.

[5] Gutman, G.J. and Schwerdtfeger, W.: The role of latent and sensible for the development of a high pressure system over the subtropical Andes in the summer. Meteorol. Rundch., 18, 69-75, 1965.

[6] Gray and Jacobson: Diurnal variations of deep cumulus convection. Mon. Wea. Rev., 105, 1171-1188, 1977.

[7] Haltiner, G.J.: Numerical weather prediction. New York: John Wiley & Sons, Inc., 317 pp., 1971.

[8] Hastenrath, S. and Heller, L.: Dynamics of hazards in Northeast Brazil. Quart. J. Roy. Meteor. Soc., 103, 77-92, 1977.

[9] Kasahara, A. and Mizzi, A.: Temporal variations of the divergence field in the E.C.M.W.F. level III-B analysis data. National Center of Atmospheric Research. P.O. Box 3000, Boulder, Co. 80.307, 1984.

[10] Kidson, J.W.: Tropical eigenvector analysis and Southern Oscillation. Mon. Wea. Rev., 103, 187-196, 1975.

[11] Kousky, V.E.: Frontal influences on northeast Brazil. Mon. Wea. Rev., 107, 1140-1153, 1979.

[12] Kousky, V.E., M. Kagano and I.F.A. Cavalcanti: The Southern Oscillation: oceanic-atmospheric circulation changes and related rainfall anomalies. Accepted in Tellus, 1983.

[13] Kruels, R., Fraedrich and E. Ruprecht: An aerological climatology over South America. Meteor. Rundsch., 28, 17-24, 1975.

[14] Lau, K.M. and H. Lim: On the dynamics of equatorial forcing of climate telecommunications. J. Atmos. Sci., 41, 161-176, 1984.

[15] Moura, A.D. and Shukla, J.: On the dynamics of droughts in Northeast Brazil: Observations, theory and numerical experiments with a general circulation model. J. Atmos. Sci., 38, 2653-2675, 1981.

[16] Namias, J.: Influence of northern hemisphere general circulation on drought in Northeast Brazil. Tellus, 24, 336-343, 1972.

[17] Riehl, H.: Climate and weather in the tropics. London, Academic Press, 611pp., 1979.

[18] Salby, M.L., D.L. Hartmann, P.L. Bailey and J.C. Gille: Evidence for equatorial Kelvin modes in Nimbus-7 LIMS. J. Atmos. Sci., 41, 220-235, 1984.

[19] Silva Dias, P.L., W.H. Scubert and M. DeMaria: Large-scale response of the tropical atmosphere to transient convection. J. Atmos. Sci., 40, 2689-2707, 1983.

[20] Silva Dias, P.L., J.P. Bonati and V.E. Kousky: Diurnally forced tropical tropospheric circulation over South America. Submitted to Mon. Wea. Rev., 1985.

[21] Virji, J.: A preliminary study of summertime tropospheric circulation patterns over South America from cloud winds. Mon. Wea. Rev., 109, 599-610, 1981.

[22] Virgi, H. and Kousky, V.E.: Regional and global aspects of a low latitude frontal penetration in Amazonas and associated tropical activity. Paper presented at the First International Conference on Southern Hemisphere Meteorology. São Josē dos Campos, SP, Brazil, 1983.

Author's address: Dr. Prof. Pedro L. da Silva Dias, Departmento de Meteorologia, Universidade de Sao Paulo - USP, Caixa Postal 30627, 01051 Sao Paulo, S.P. Brazil.

Figure Legends

Fig. 1a - Infrared satellite image for 01/05/81 at 21:16 GMT. (SMS-2).

Fig. 1b - 200mb streamlines (solid lines with arrows) and 500mb vertical motion in $10^{-4}mbs^{-1}$ on 01/06/81 at 00:GMT.

Fig. 2 - Infrared satellite image of (a) 01/23/81 at 12:16 GMT (SMS-2), (b) 01/23/81 at 21:16 GMT, (c) 01/24/81 at 12:16 GMT, (d) 01/24/81 at 21:16 GMT, (e) 01/25/81 at 09:16 GMT, (f) 01/25/81 at 21:17 GMT.

Fig. 3 - 200mb wind vectors and vertical motion in pressure coordinate in $10^{-4}mbs^{-1}$ (sinking motions are represented by dashed lines and upward motion, by sollid lines) on (a) 01/23/81 at 00:GMT (Vmax = 66 m/s), (b) 01/23/81 at 12:GMT (Vmax = 71 m/s), (c) 01/24/81 at 00:GMT (Vmax = 77 m/s), (d) 01/24/81 at 12:GMT (Vmax = 72 m/s), (e) 01/25/81 at 00:GMT (Vmax = 75 m/s), (f) 01/25/81 at 12:GMT (Vmax = 68 m/s).

Fig. 4 - Time dependence of heat source. Tmax = 24 hours in the model computations.

Fig. 5 - Wind flow at 250mb after 24 hours for a heat source centered at 10^{o}S and 60^{o}W with symmetrical e-folding width of 1500 km. Maximum vector corresponds to $1.98ms^{-1}$.

Fig. 6 - Same as Fig. 5 but at 48 hours. Vmax = $4.94ms^{-1}$.

Fig. 7 - Vertical p-velocity in $10^{-4}mbs^{-1}$ at 500mb after 24 hours.

Fig. 8 - Same as Fig. 7 but after 48 hours.

Fig. 9 - Same as Fig. 7 but for a heat source centered at 15^{o}S and zonal

e-folding width of 700 km and meridional width of 1500 km.

Fig. 10 - Same as Fig. 5 but at 48 hours for realistic initial flow. Vmax = 19.82 ms^{-1}.

Fig. 11 - Difference between 250mb wind field at 48 hours and initial flow. Vmax = 4.96 ms^{-1}.

Fig. 12 - Vertical p-velocity in $10^{-4}mbs^{-1}$ at 48 hours for a heat source located at the Equator and $130^{O}W$.

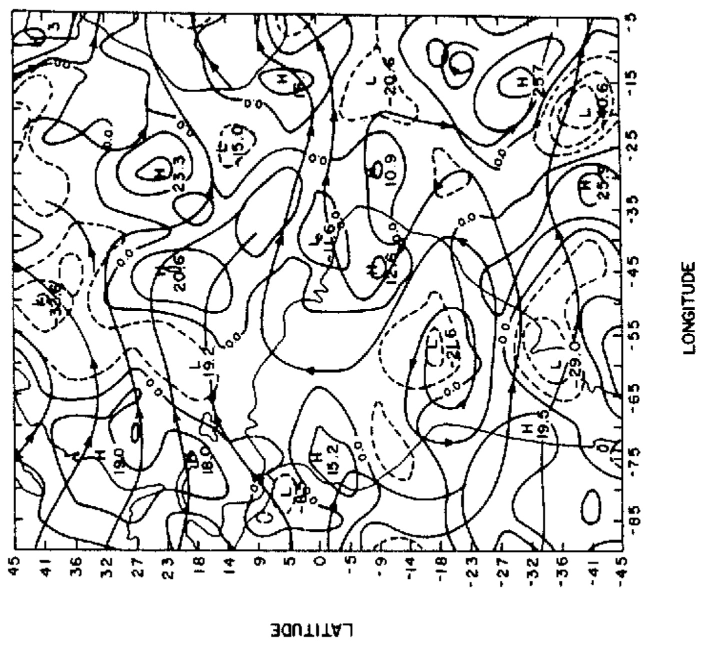

Fig. 1b

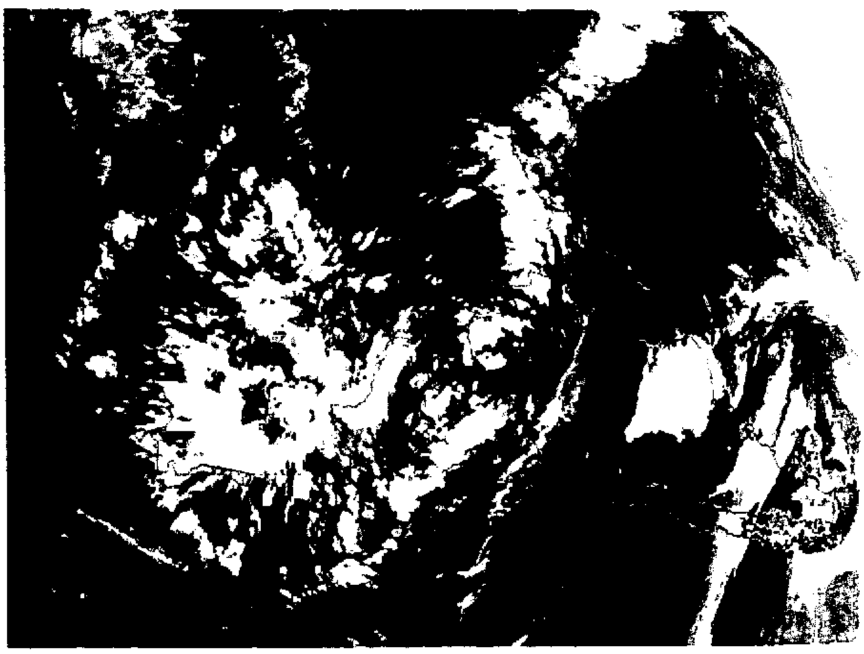

Fig. 1a

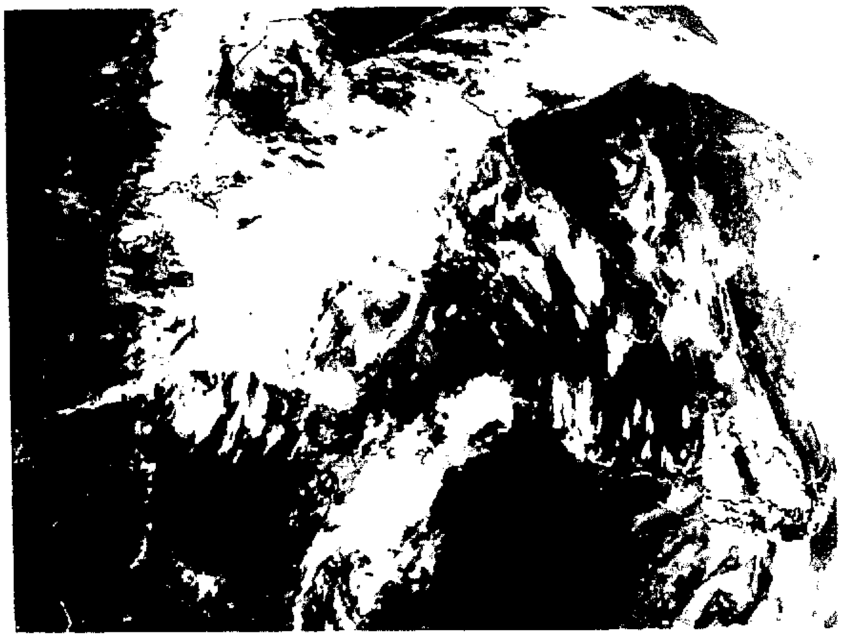

Fig. 2b

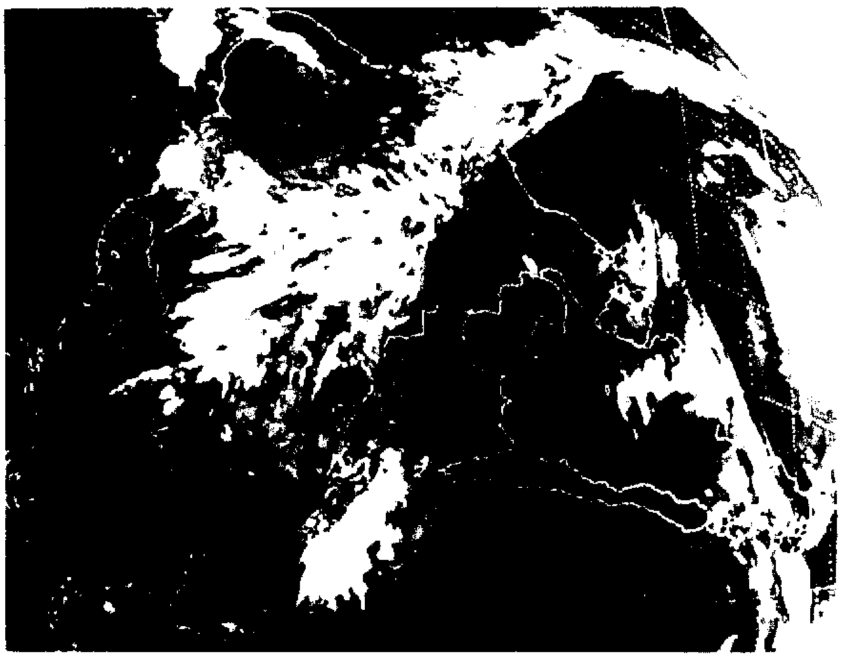

Fig. 2a

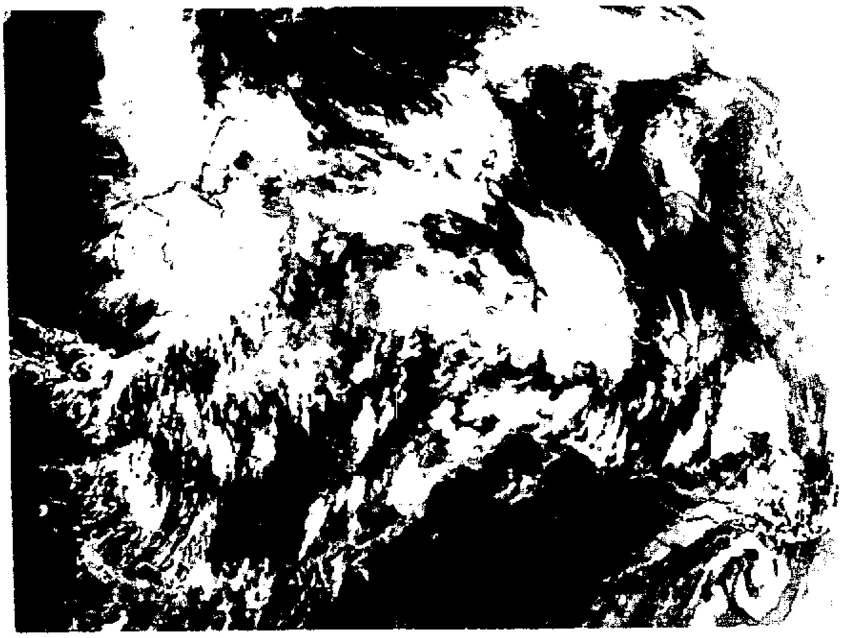

Fig. 2d

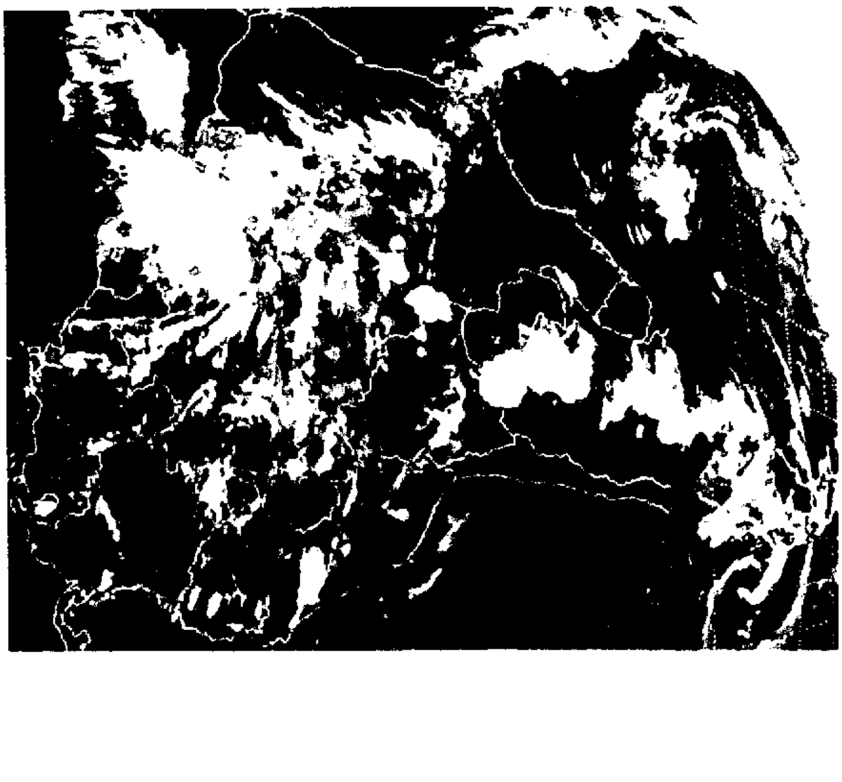

Fig. 2c

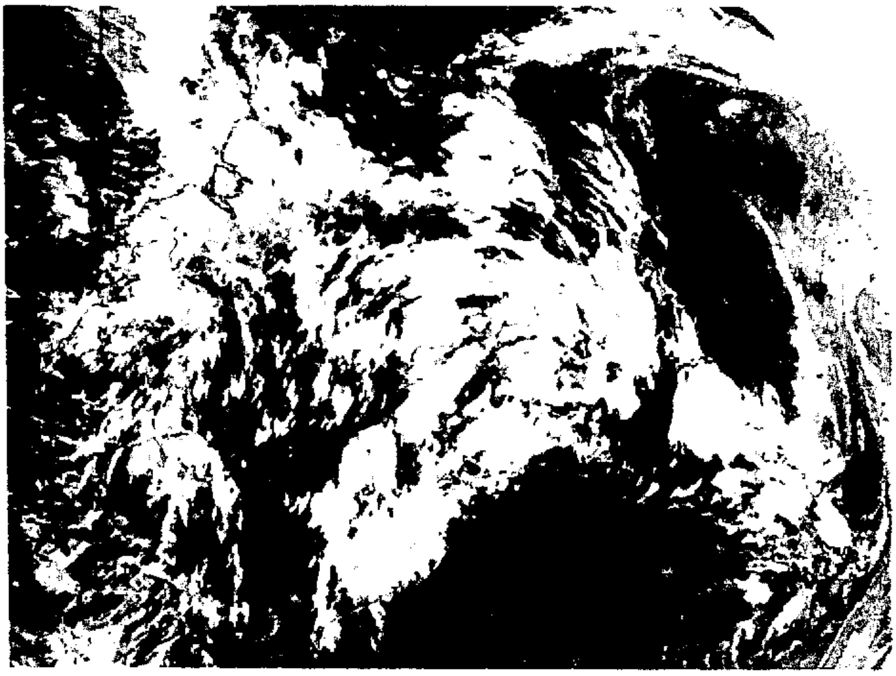

Fig. 2f

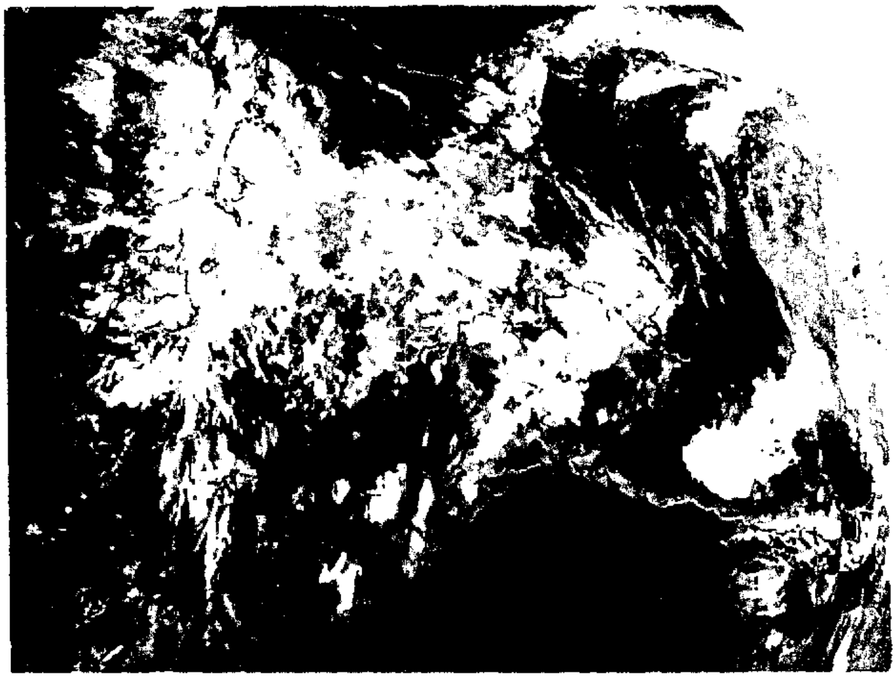

Fig. 2e

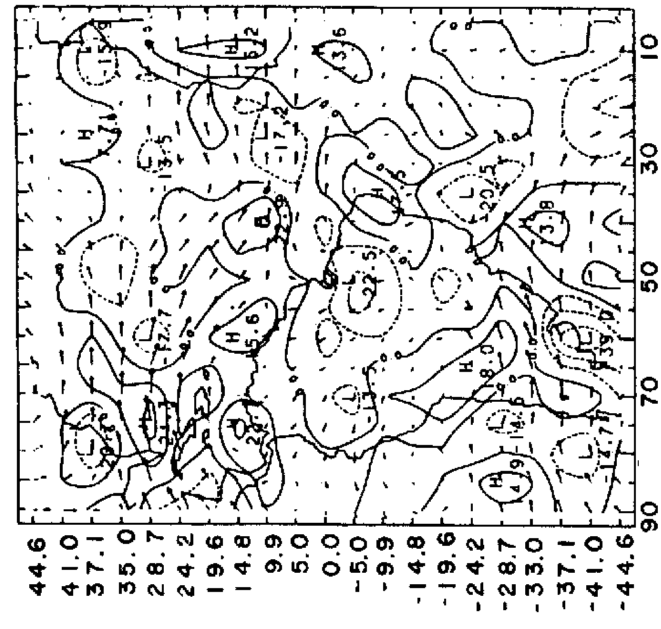
44.6
41.0
37.1
35.0
28.7
24.2
19.6
14.8
9.9
5.0
0.0
-5.0
-9.9
-14.8
-19.6
-24.2
-28.7
-33.0
-37.1
-41.0
-44.6
90
70
50
30
10

Fig. 3b

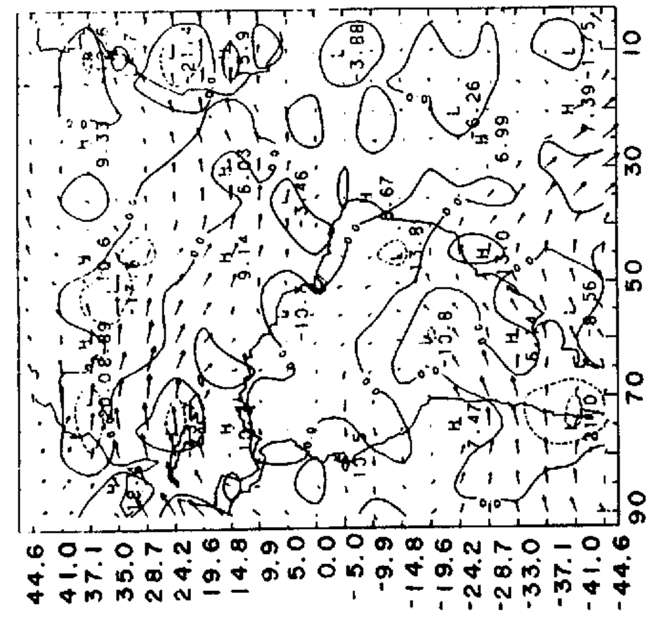
44.6
41.0
37.1
35.0
28.7
24.2
19.6
14.8
9.9
5.0
0.0
-5.0
-9.9
-14.8
-19.6
-24.2
-28.7
-33.0
-37.1
-41.0
-44.6
90
70
50
30
10

Fig. 3a

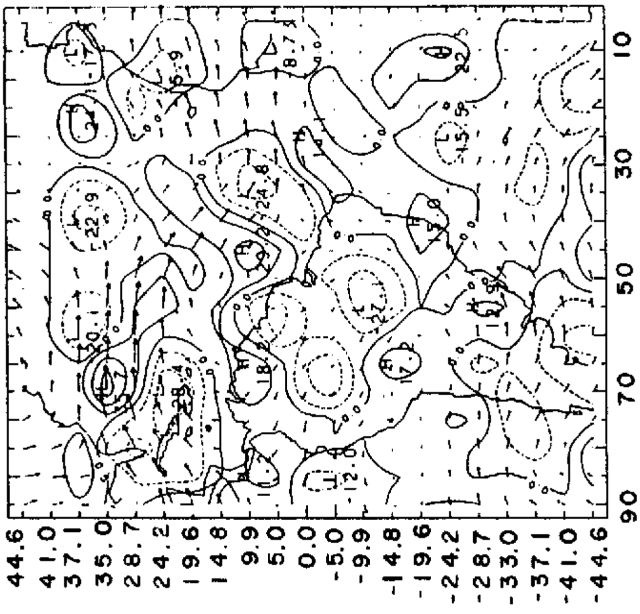
44.6
41.0
37.1
35.0
28.7
24.2
19.6
14.8
9.9
5.0
0.0
-5.0
-9.9
-14.8
-19.6
-24.2
-28.7
-33.0
-37.1
-41.0
-44.6
90
70
50
30
10

Fig. 3d

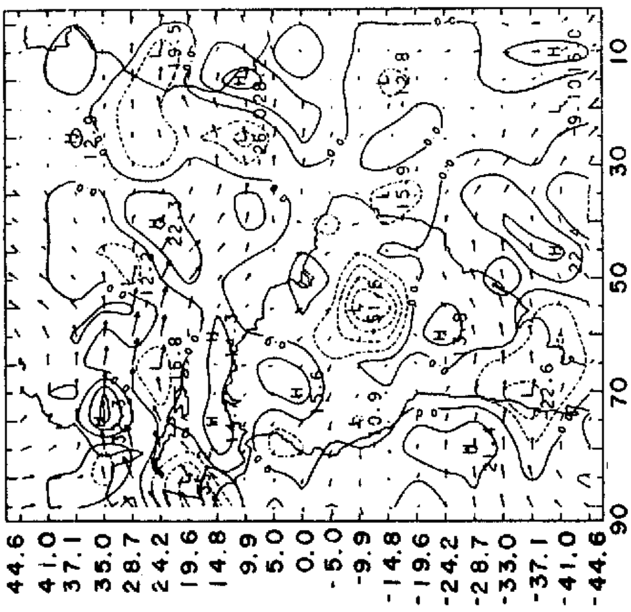
44.6
41.0
37.1
35.0
28.7
24.2
19.6
14.8
9.9
5.0
0.0
-5.0
-9.9
-14.8
-19.6
-24.2
-28.7
-33.0
-37.1
-41.0
-44.6
90
70
50
30
10

Fig. 3c

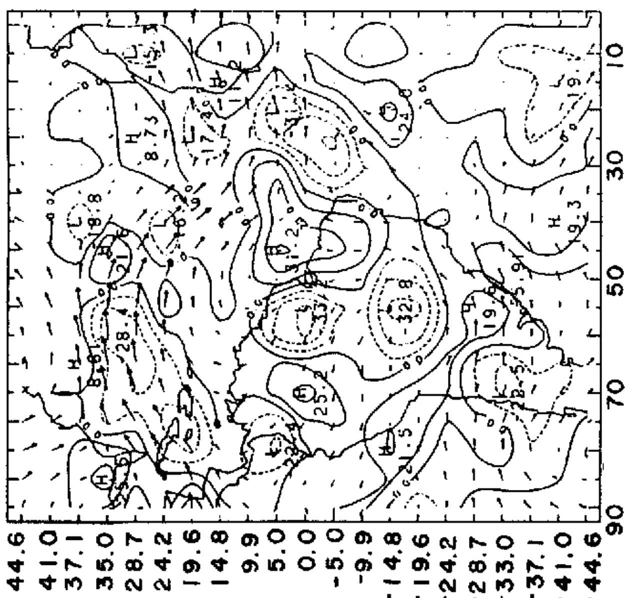
44.6
41.0
37.1
35.0
28.7
24.2
19.6
14.8
9.9
5.0
0.0
-5.0
-9.9
-14.8
-19.6
-24.2
-28.7
-33.0
-37.1
-41.0
-44.6
90
70
50
30
10

Fig. 3e

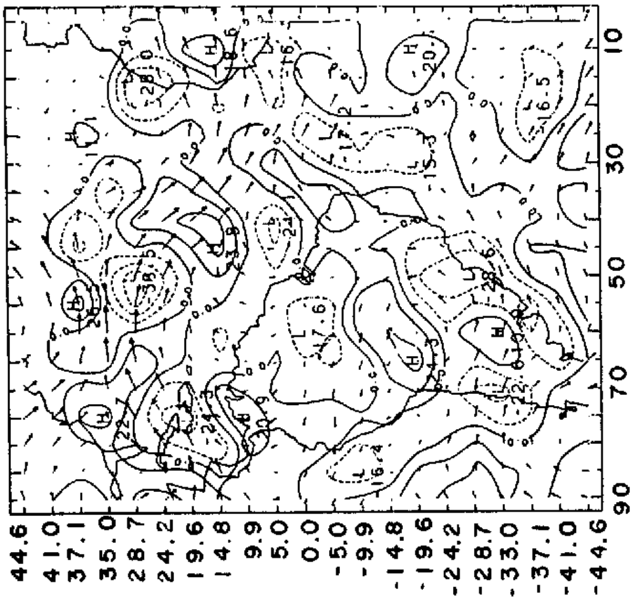
44.6
41.0
37.1
35.0
28.7
24.2
19.6
14.8
9.9
5.0
0.0
-5.0
-9.9
-14.8
-19.6
-24.2
-28.7
-33.0
-37.1
-41.0
-44.6
90
70
50
30
10

Fig. 3f

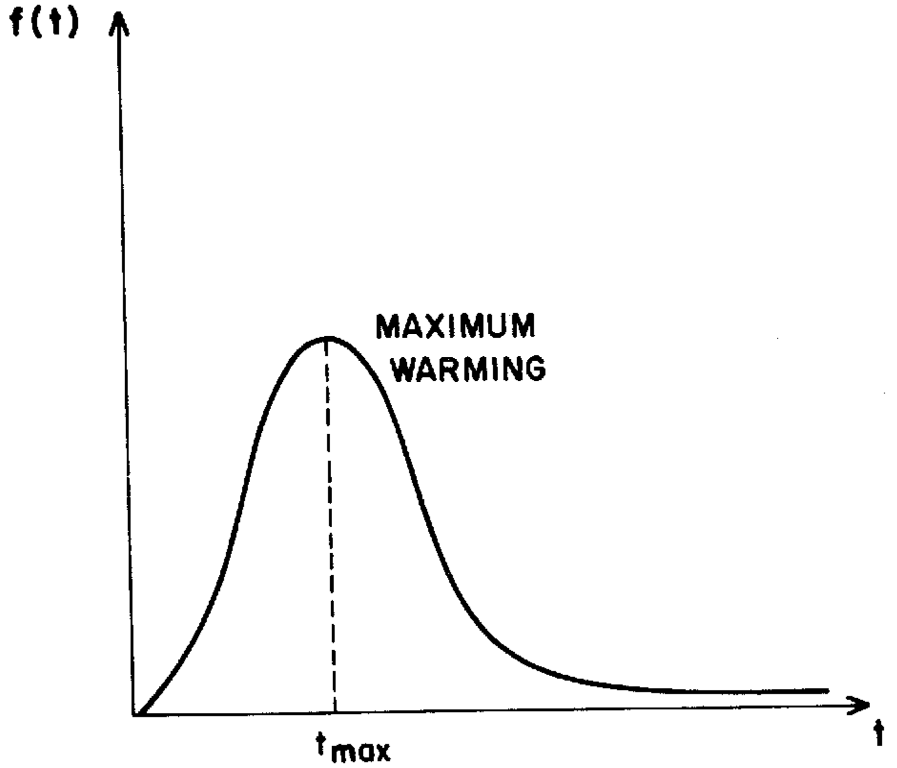

Fig. 4

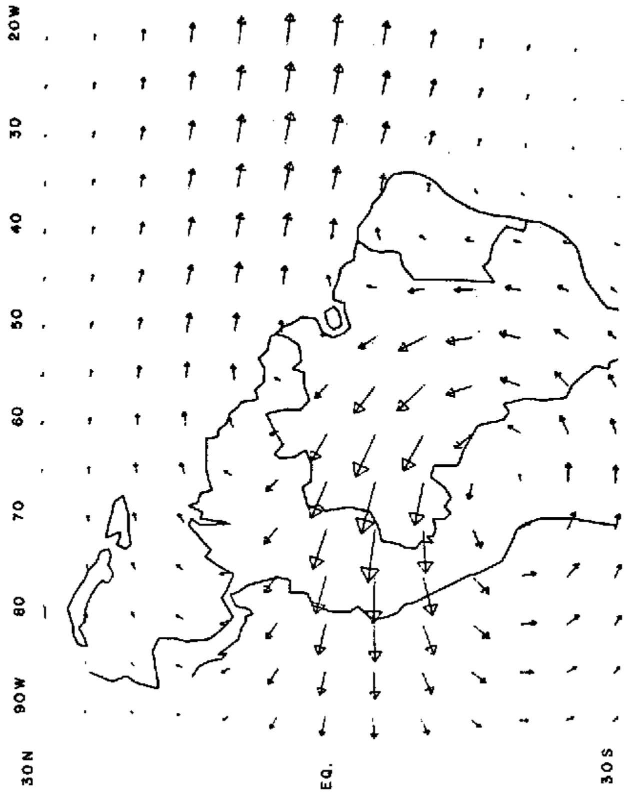
20W
30
40
50
60
70
80
90W
30N
EQ.
30S

Fig. 6

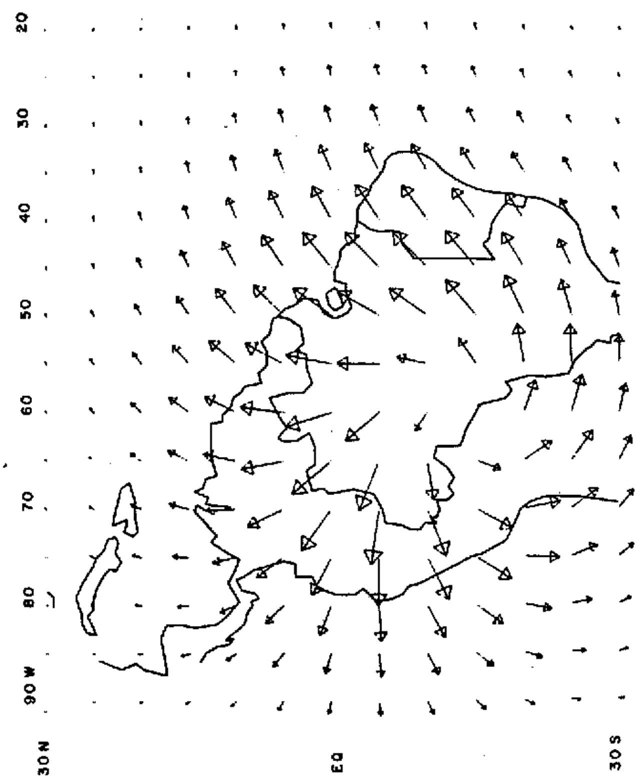
20
30
40
50
60
70
80
90W
30N
EQ
30S

Fig. 5

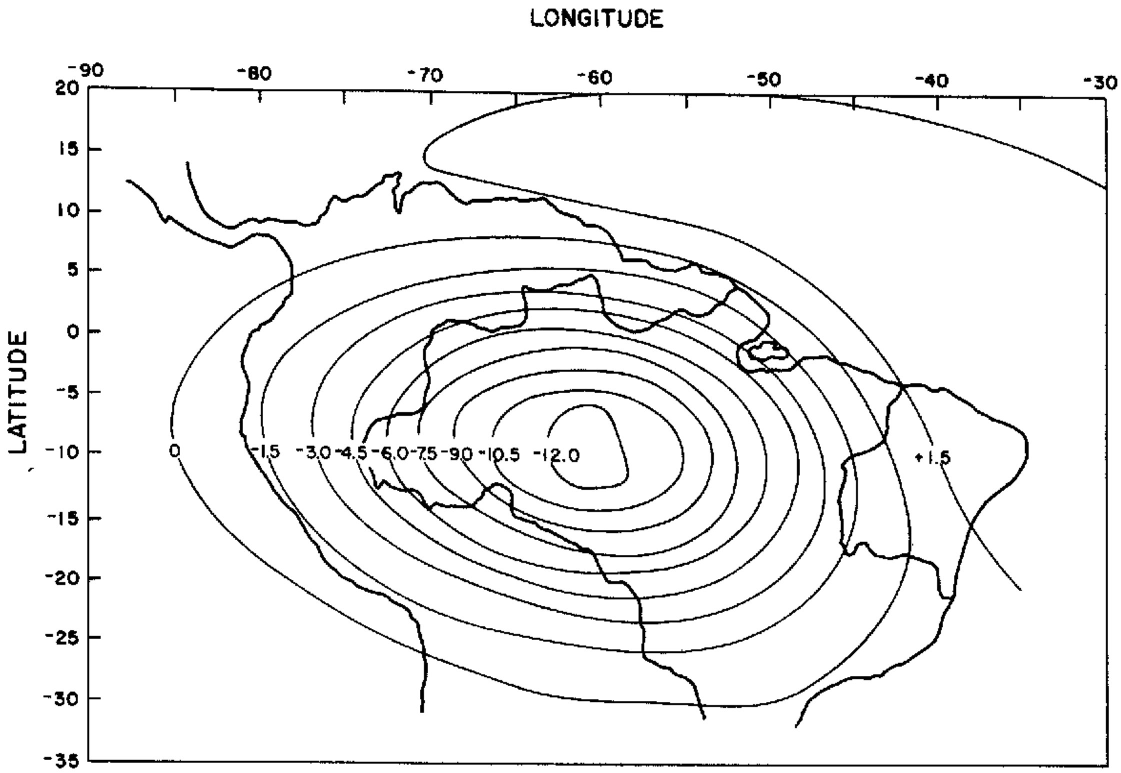
LONGITUDE
-90
-80
-70
-60
-50
-40
-30
20
15
10
5
0
-5
-10
-15
-20
-25
-30
-35
LATITUDE
0
-1.5
-3.0
-4.5
-6.0
-7.5
-9.0
-10.5
-12.0
+1.5

Fig. 7

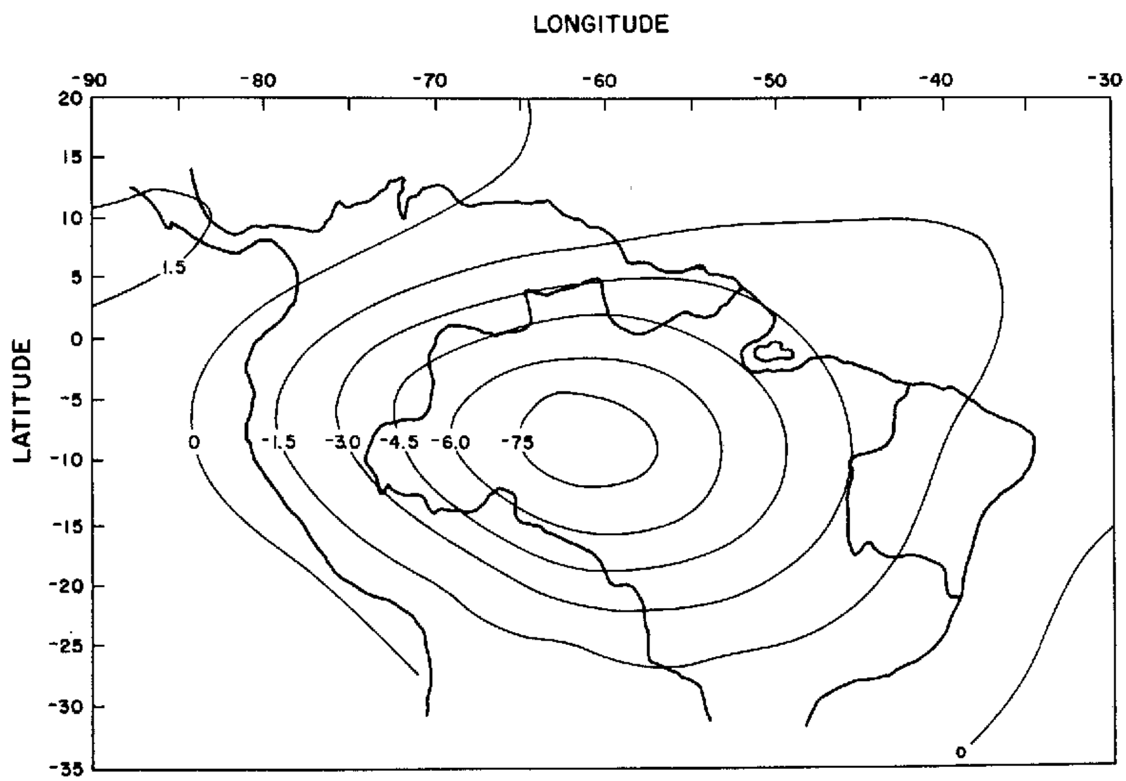
LONGITUDE
-90
-80
-70
-60
-50
-40
-30
20
15
10
5
0
-5
-10
-15
-20
-25
-30
-35
LATITUDE
1.5
0
-1.5
-3.0
-4.5
-6.0
-7.5
0

Fig. 8

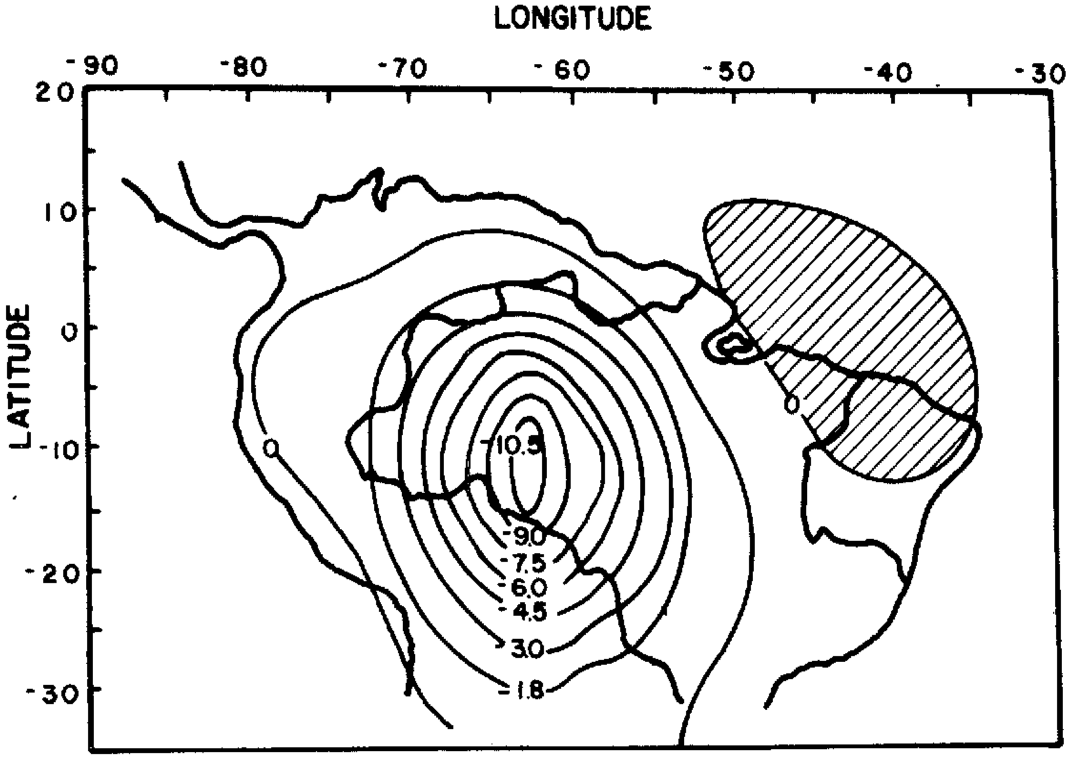
LONGITUDE
-90
-80
-70
-60
-50
-40
-30
20
10
0
-10
-20
-30
LATITUDE
0
0
-10.5
-9.0
-7.5
-6.0
-4.5
-3.0
-1.8

Fig. 9

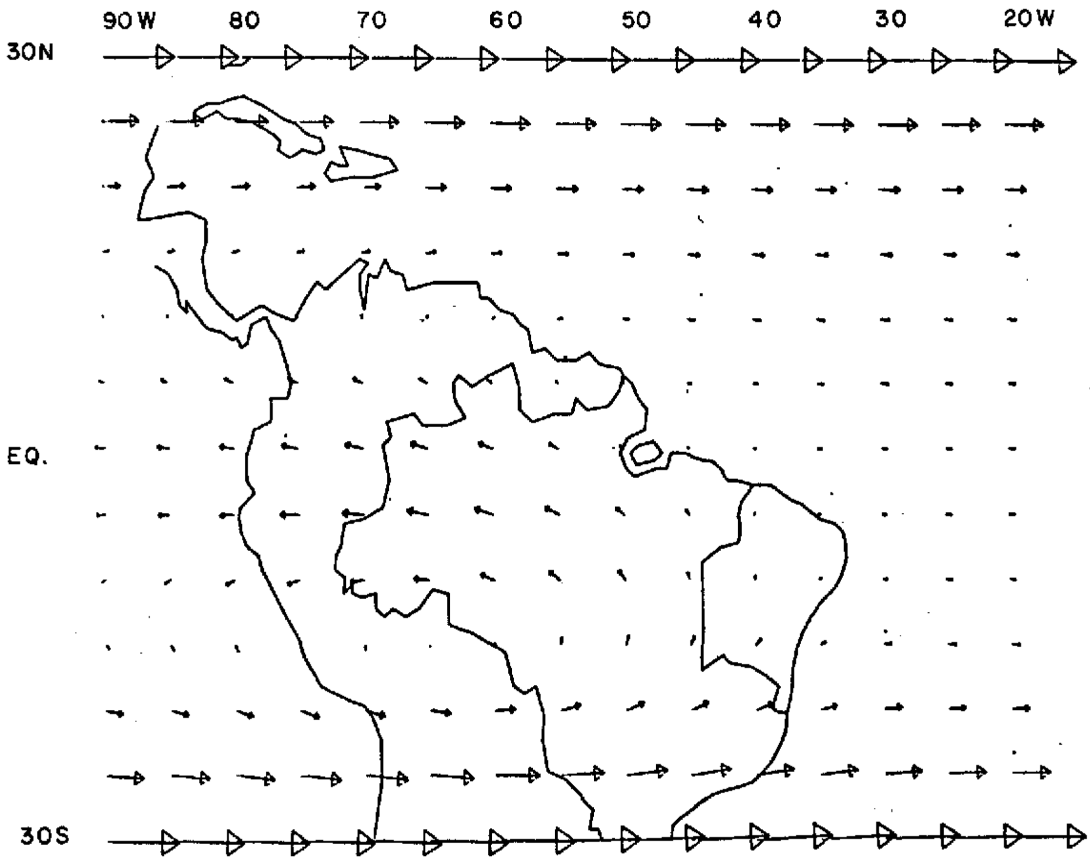
90W
80
70
60
50
40
30
20W
30N
EQ.
30S

Fig. 10

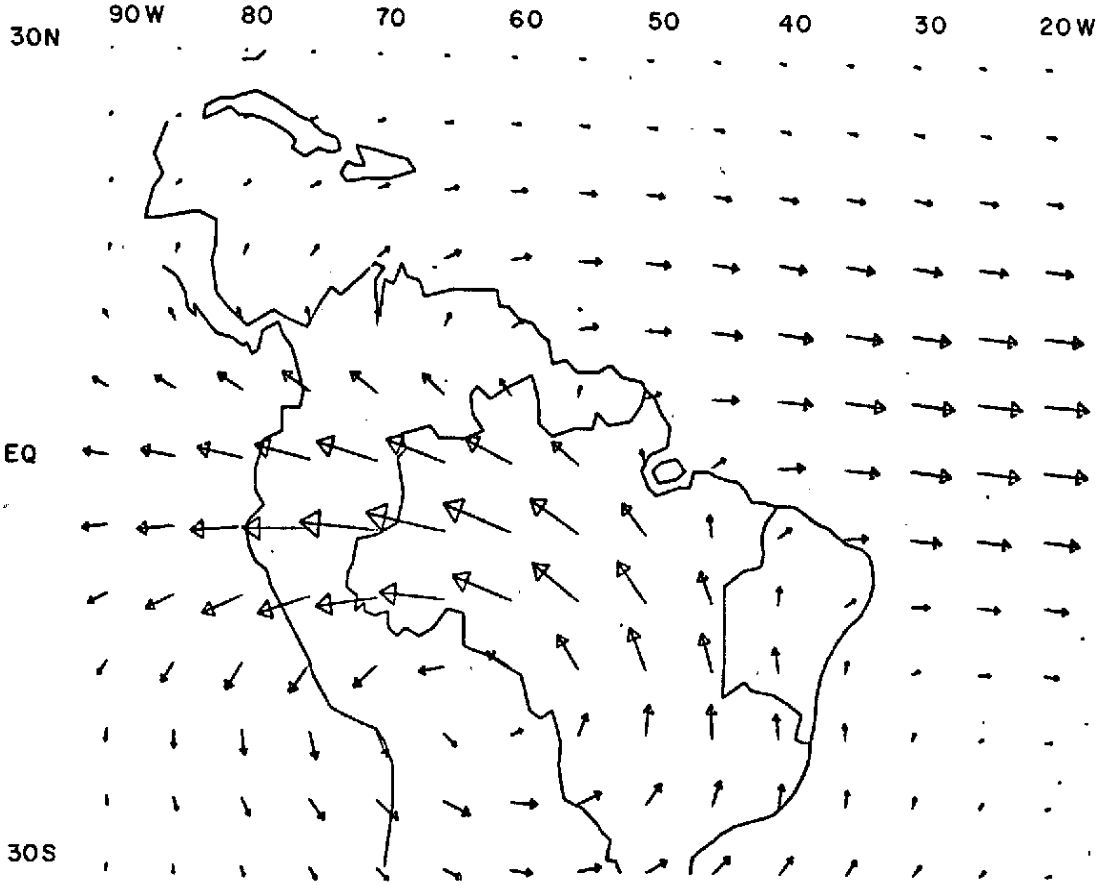
90W
80
70
60
50
40
30
20W
30N
EQ
30S

Fig. 11

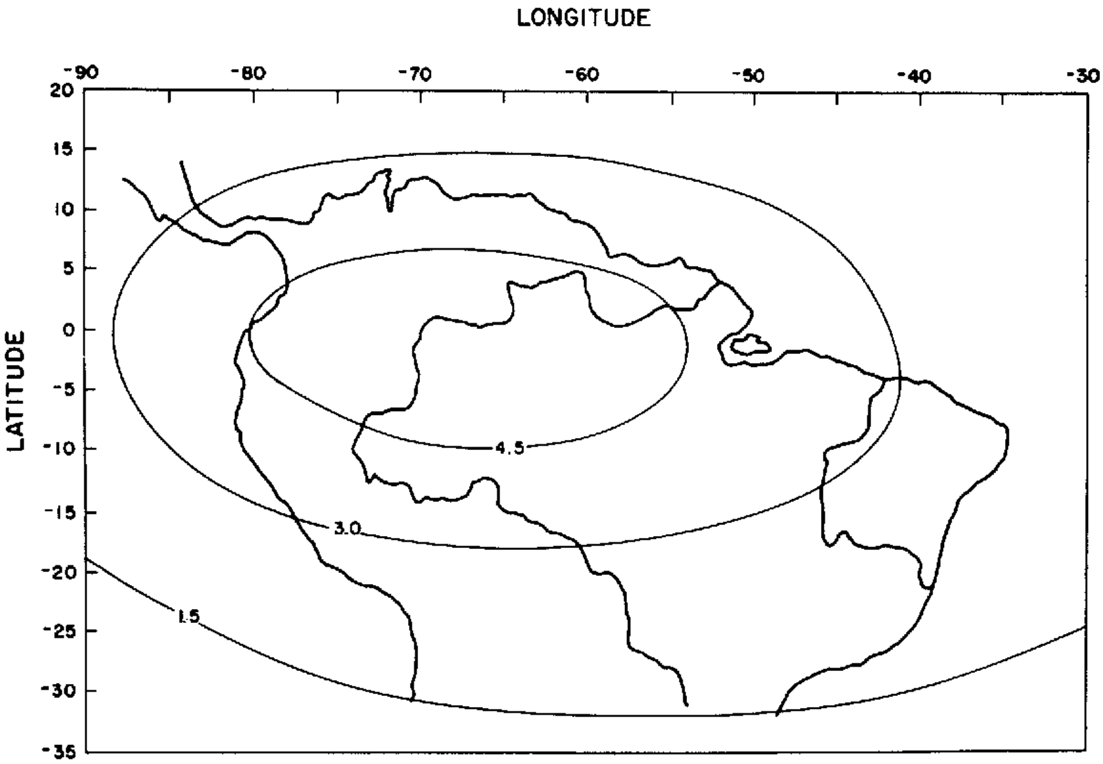
LONGITUDE
-90
-80
-70
-60
-50
-40
-30
LATITUDE
20
15
10
5
0
-5
-10
-15
-20
-25
-30
-35
4.5
3.0
1.5

Fig. 12